GMR
The Original

MID-INFRARED SPECTROSCOPIC PROFILING OF HEMOLYMPH ACROSS LARVAL INSTARS IN FALL ARMYWORM, *SPODOPTERA FRUGIPERDA* (SMITH, 1797) (LEPIDOPTERA: NOCTUIDAE)

Sourabh Maheshwari[1], K.C. Sharma[1*], S.K. Jain[1], Priyanka Meena[1], Purnima Kekti[1,2], Geeta Songer[1,2], Tekchand Nayak[1,2], Hem Prakash Verma[1] and P.K. Rai[1]

[1]ICAR-National Institute of Biotic Stress Management, Raipur, Chhattisgarh-493225, India
[2]Department of Entomology, College of Agriculture, Indira Gandhi Krishi Vishwavidhyala, Raipur, Chhattisgarh-492012, India
***Corresponding author:** Email: kcbhuvan2004@gmail.com

ABSTRACT
The circulatory system in insects serves an essential role in coordinating physiological processes, particularly homeostasis, defense, heat transfer and gaseous exchange. Hemolymph acts as functional analogue to vertebrate blood and lymph. The present study employed Attenuated Total Reflectance–Fourier Transform Infrared (ATR-FTIR) spectroscopy to characterize hemolymph biochemical composition of fall armyworm (*Spodoptera frugiperda*) larvae across third, fourth, and fifth instars. Hemolymph samples collected from thoracic region were analyzed in mid-infrared region (4000-400 cm^{-1}). Changes in corresponding wavenumber along with functional groups and molecular vibrations revealed instar-specific variations in crucial biomolecules comprising carbohydrates, proteins, lipids and nucleic acids. The single bond region (3700–3300 cm^{-1}) corresponds to progressive elevation in hydroxyl and amide A bands, indicating accelerating hydration and protein concentration during larval development. The double bond region (1750–1500 cm^{-1}) exhibited distinct carbonyl (C=O) and amide I and II peaks, reflecting increased lipid deposition and protein synthesis for subsequent utilization in later stages (pupal and adult development). Carbohydrate and phospholipid signals in the fingerprint region (1500–600 cm^{-1}) reflect biochemical complexity associated with larval growth and development. These distinct age-related spectral patterns demonstrate compositional shifts across each developmental instar, establishing ATR-FTIR spectroscopy as a rapid, non-damaging, reagent-free tool capable of identifying age-specific changes in biochemical complexities for precise assessment in *S. frugiperda* larvae.

KEYWORDS: FTIR spectroscopy, biochemical profiling, larval development, mid-infrared region, *Spodoptera frugiperda*

1. INTRODUCTION

Fourier transform infrared (FT-IR) spectroscopy, specifically in the mid-infrared region (MIR) most widely utilized technique in entomological research for more than six decades (Johnson and Naiker, 2020a). It serves as powerful analytical tool for qualitative and quantitative resolution of biochemical components in insect tissues and body fluids (Johnson and Naiker, 2020b). This technique has potential application in the profiling of cuticular hydrocarbons (Bagneres and Wicker-Thomas, 2010; Gibbs and Crowe, 1991), taxonomic discrimination of cryptic species (Johnson, 2020), sex discrimination (Khoshmanesh et al., 2017), age prediction (Johnson and Naiker, 2020b), biotype discrimination (Teixeira et al., 2015), endosymbiont detection (such as Wolbachia) (Khoshmanesh et al., 2017), hemolymph analysis (Horvatinec and Svečnjak, 2020), and characterization of cuticular surface chemistry of different body parts of insect (Teixeira et al., 2015), and products (Boulet-Audet et al., 2015). The FT-IR spectroscopy assists in the detection of functional groups (e.g., -COOH, -C≡C-, -CH3, -C≡O-, $-NH_2$) by absorbing infrared radiation (IR) at a specific wavenumber, producing a characteristic spectral pattern (Johnson and Naiker, 2020a). The IR spectrum is distributed into three major bands: the far-IR spectrum (400 cm^{-1} - 50 cm^{-1}; or 25 µm -200 µm), the mid-IR spectrum (4000 cm^{-1} - 400 cm^{-1}; or 2500 nm - 25,000 nm), and the near-IR spectrum (14,000 cm^{-1}- 4000 cm^{-1}; or ~710 nm - 2500 nm) (Rodriguez-Saona and Allendorf, 2011). The mid-IR region (4000 cm^{-1}- 400 cm^{-1}) is most extensively utilized range of the infrared spectrum, where absorption bands are represented concerning wavenumber (measured in cm^{-1}). The ATR-FTIR algorithm captures the entire mid-IR spectrum at once, measuring all wavelengths simultaneously through interferometric modulation to achieve high spectral resolution. The MIR region is highly sensitive to the mechanical motion of atoms linked by a covalent bond within biological macromolecules, including their characteristic vibrational and rotational modes. The modes of vibration include symmetric stretch and asymmetric stretch, along with bending motions (scissoring, wagging, rocking, and twisting). Each vibration has a characteristic frequency determined by the bond type, its transitional energy levels, and the mass of atoms involved in bond formation (Johnson and Naiker, 2020a). The MIR spectrum, therefore, exhibits highly specific and distinctive absorption peaks corresponding to different

chemical bonds, enabling for quantitative and also semi-quantitative estimation of various functional groups found in sample matrix (Cozzolino, 2014; Johnson et al., 2019).

Insects, like other organisms, rely on a complex biochemical system for metabolism, growth, and immune defense (Browne et al., 2013). The hemolymph acts as a functional equivalent of blood in insects. It is a transparent or slightly yellowish fluid circulating within their open circulatory system. It consists of water, inorganic ions, sugars, lipids, amino acids, proteins, and free-floating hemocytes. Hemolymph plays a crucial role in nutrient transport, osmoregulation, detoxification, wound healing, and immune responses. The immune framework of insects composed of both cellular and humoral building blocks (Lavine and Strand, 2002). Cell- mediated immunity carries out defensive actions such as phagocytosis, encapsulation, and coagulation, while humoral defenses depend on soluble immune factors such as antimicrobial peptides (AMPs), complex proteins, melanin precursors, and phenol oxidase cascade products that work together to neutralize invading pathogens (Gupta, 2019; Wang et al., 2017).

The fall armyworm (*Spodoptera frugiperda*) is a highly polyphagous noctuid pest for global agricultural productivity, causing severe yield losses in maize (*Zea mays* L.) and several other crops. Its ability to rapidly reproduce, long-distance migration, and adaptability to diverse agroecological conditions make it a challenging pest to manage (Tay et al., 2023). Understanding its biochemical and physiological mechanisms, particularly through hemolymph analysis, can provide valuable insights into its development, metabolism, immune functions, and responses to various biotic and abiotic stressors or agents (Eleftherianos et al., 2021). Most previous studies on insect hemolymph have focused on quantifying specific biochemical constituents such as Carbohydrates, lipids, or proteins, and the use of spectroscopic tools remains limited (Mullins, 2013). MIR spectroscopy serves as rapid, non- destructive, reagent-independent analytical method (Ellis et al., 2003) for biochemical studies of insect hemolymph (Horvatinec and Svečnjak, 2020). Therefore, preset study intended to characterize the biochemical composition of hemolymph from various development stages (third, fourth and fifth instar larvae) of *S. frugiperda* using mid-infrared spectroscopy. The technique was employed to detect and compare biochemical changes across successive larval instars by analyzing the spectral fingerprints corresponding to functional groups such as proteins (amide I and II), lipids (CH_2 and C=O), Carbohydrates (C-O), and phosphate compounds (PO^{2-}). The study elucidates instar-specific variation in hemolymph composition that reflect the physiological and metabolic transitions occurring during larval development.

2. MATERIALS AND METHODS

Fall armyworm (*S. frugiperda*) insect were gathered from maize fields infested with larvae and reared within laboratory following Maranabasari et al. (2024) with minor modifications. Larvae were reared in plastic containers under controlled conditions of 27 ± 2 °C temperature, 70–80% RH and 14:10 h light: dark photoperiod. Fresh maize leaves were supplied daily to larvae until pupation, and containers were cleaned regularly to prevent microbial contamination. Pupae were shifted to plastic jars lined with wet filter paper to support adult emergence after pupation. Emerged adult moths were released into oviposition cages fed with a 10% honey solution as a food source. Maize seedlings were provided as oviposition substrates, and the egg masses obtained were used to establish a continuous laboratory culture. Larval instars (3rd, 4th, and 5th instars) feeding on maize leaves were identified according to the biological lifecycle of FAW described by Kalleshwaraswamy et al. (2018) based on biology (head capsule width measurements, body size, and observation of exuviae following molting). Hemolymph was collected as per the protocol suggested by Paikra and Mishra (2019) from F1 generation larvae at the 3rd, 4th, and 5th instars. Approximately ~6-8 µL of hemolymph was gently drawn from each larva by puncturing the thoracic region using a sterile needle (to avoid contamination with gut contents as well as excessive stress to larvae). Freshly collected hemolymph was immediately transferred onto a diamond crystal of the ATR-FTIR spectrometer. Spectra recorded at room temperature (24 ± 3 °C) over a spectral resolution of 4000- 400 cm-1 using 4 cm-1 resolution. For each sample, 32 scans were averaged to improve signal-to-noise ratio. An automated ATR correction was applied through the instrument software. The IR spectra bands of hemolymph were interpreted as suggested by Coates (2000) and Nandiyanto et al. (2019).

3. RESULTS AND DISCUSSION

ATR-FTIR spectra of 3rd-, 4th-, and 5th-instar *S. frugiperda* larvae hemolymph from 4000-400 cm-1 revealed distinct variations in functional groups as summarized in Table 1 and shown in Figure 1 (a-c). These spectral differences correspond to shifts in ontogenic patterns of development and changes in major biomolecules such as proteins, lipids, carbohydrates, and amides. In the single bond region (2500-4000 cm^{-1}) of the mid-IR spectrum, a wide absorption band between 3700-3300 cm^{-1}, assigned to O-H and N-H stretching modes of vibration. The hydroxyl (-OH) stretching peak appeared at 3836.67, 3836.67, and 3924.26 cm^{-1} at the 3rd, 4th, and 5th instar, respectively, indicating increased free hydroxyl groups and higher metabolic hydration in later instars. Peaks around 3600-3800 cm^{-1} corresponded to Amide A (-NH) stretching, confirming protein-rich hemolymph, suggesting elevated protein content with peaks at 3801.08, 3800.92, and 3899.43 cm^{-1} at the 3rd, 4th, and 5th instar, respectively. It also indicates that the 5th instar larvae showed enhanced water-bound amide structures, reflecting a higher physiological demand for pre-pupal development. Additionally, characteristic peaks corresponding to free -OH and H-bonded -OH stretching modes of vibration were noticed in the 3500-3700 cm^{-1} region at 3742.40, 3742.45, and 3836.76 cm^{-1} for the 3rd, 4th, and 5th instar, respectively. Similarly, peaks

recorded in the 3300-3700 cm^{-1} at 3671.26, 3671.10, and 3801.00 cm^{-1} at the 3rd, 4th, and 5th instar, respectively, were also indicative of -OH stretching. Notably, spectra in 3400-3500 cm^{-1} and 3200- 3400 cm^{-1} range absorption bands appeared exclusively in 5th instar at 3742.31 and 3671.37, respectively, suggesting enhanced hydrogen bonding and higher water content at this stage. Furthermore, peaks in the 3200-3300 cm^{-1} region at 3284.47, 3309.54, and 3312.99 cm^{-1} in the 3rd, 4th, and 5th instar, respectively, correspond to -NH stretching (protein), -OH bending vibrations of water and sugars. In triple bond region (2000-2500 cm^{-1}), peaks were observed in all stages at 2119.36, 2109.73, and 2120.00 cm^{-1}, in the 3rd, 4th, and 5th instar, respectively, attributed to C≡C, indicating the presence of unsaturated hydrocarbons and minor lipid components. No major variations were observed across instars in the triple bond region.

Within the double bond spectra region (1500-2000 cm^{-1}), peaks seen at 1867.06, 1867.09, and 1867.21 cm^{-1} in the 3rd, 4th, and 5th instar, respectively, correspond to the combination region. The characteristic carbonyl stretching modes of vibrations in the range of 1700-1750 cm^{-1}, particularly at 1749.34, 1749.51, and 1749.39, in the 3rd, 4th, and 5th instar, respectively, are imputed to -C=O ester stretching, indicating presence of lipids and phospholipids in the hemolymph samples. Further, peaks in the 1600-1700 cm-1 region at 1643.56, 1643.09, and 1643.62 cm^{-1} show amide I for -C=O- stretch in protein-bound water. In the range 1500- 1600 cm^{-1}, peaks at 1559.91, 1559.87, and 1559.85 cm^{-1} show amide II for N-H bend and - C-N- stretch. No major variations were observed across instars in the double bond region.

The fingerprint spectra region (600-1500 cm^{-1}) of ATR-FTIR revealed characteristic absorption peaks related to key biomolecular functional groups in the hemolymph of *S. frugiperda* larvae across the 3rd, 4th, and 5th instar, peaks observed at 1523.40, 1523.41, and 1523.36 cm^{-1} were imputed to C-C stretching (aromatic) and CH_2 bending modes of vibrations, including the presence of aliphatic hydrocarbons associated with structural biomolecules. The absorption bands near 1396.72-1396.62 cm^{-1} corresponded to symmetric stretching of -COO groups derived from amino acids and fatty acids, representing the amide functional group. Peaks between 1367.49 and 1367.62 cm^{-1} showed C-H bending vibrations associated with Amide III bands, which indicate tertiary amides that aid in secondary structures of protein. The biochemical contribution of phospholipids and carbohydrates like trehalose and symmetric PO^{-2} stretching vibrations of nucleic acids and phospholipids was featured by additional stretching vibrations between 1167.47-1172.06 cm^{-1} that were associated with C-O and PO^{-2} groups, usually originating from phospholipids and sugar moieties. The C-O stretch of carbohydrates (trehalose) is represented by peaks between 1089.20 and 1088.96 cm^{-1}, while nucleic acids and phospholipids are represented by the PO^{-2} symmetric stretch.

Collectively, these spectra confirm the biochemical complexity of larval hemolymph, revealing the existence of protein, lipids, carbohydrates, nucleic acid derivatives, and phospholipids that are essential for larval growth and development. Protein plays key role in growth, cuticle synthesis, enzyme production and preparation for metamorphosis (Charles, 2010), while lipids contribute to energy storage, membrane formation, and the increased metabolic demands of pupation (Wronska et al., 2023; Akiki et al., 2024). Carbohydrates serve as the major source of energy during active feeding and metabolism (Akiki et al., 2024), whereas nucleic acid and phospholipids are involved in cellular growth and development integrity, and the regulation of developmental processes (Lehmann, 2021). Together, these biomolecules support the development progression and metabolic activity of larvae throughout successive instars (Lavine and Strand, 2002; Mullins, 2013).

Overall, the FTIR spectral changes show biochemical shift from carbohydrate-rich to protein- and lipid-rich hemolymph during larval growth and development. Carbohydrate and water-related peaks predominate in the third instar, indicating intensive feeding and energy mobilisation. An intermediate stage with balanced signals for proteins, fats, and carbohydrates is seen in the fourth instar. Protein (such as Amide I and II) and lipid (such as C=O ester and -CH_2 bending) peaks, combined with reduced carbohydrate peaks, are characteristics of the fifth instar that are compatible with energy storage prior to pupation. This shows a gradual rise in lipid-related characteristics, carbohydrate peaks (connected to trehalose), and proteinaceous components (Amide I and II). This investigation highlights the dynamic physiological changes required for proper maturation and lifecycle completion by demonstrating the substantial biochemical rearrangement of *S. frugiperda* hemolymph composition during larval development.

The present study characterises biochemical changes in the hemolymph of *S. frugiperda* larvae at various instar stages using ATR-FTIR spectroscopy. The mid-infrared (MIR) region (4000–400 cm^{-1}) exhibits distinct spectral shifts that are indicative of dynamic biochemical changes in major molecular classes, such as proteins, lipids, carbohydrates, and nucleic acids. These classes are closely associated with larval growth, metabolism, and developmental transitions. Similar uses of spectroscopic techniques, such FTIR and near-infrared spectroscopy (NIRS), have shown promise in entomological research for metabolic profile, age grading, quick species classification, and age prediction (Mwanga et al., 2019; Gonzalez-Jimenez et al., 2019; Wang et al., 2016).

The broad absorption bands in single bond spectral area (2500–4000 cm^{-1}) contributed to the O–H and N–H stretching modes of vibrations, which were mirrored by the hemolymph's protein composition and hydration state. An increase in hydroxyl group absorption from the third to the fifth instar indicates improved metabolic hydration and water binding in the latter stages. Kuroiwa et al. (2015) observed an increase in hydroxyl- and amide-absorption bands consistent with changes in water-associated and protein-related vibrations during larval development. According to reports of age-related biochemical distinction in mosquitoes using mid-infrared

spectroscopy, the fifth instar's prominent amide A peaks in the 3600–3800 cm^{-1} range indicate elevated protein synthesis and increased physiological demand prior to pupation (Gonzalez-Jimenez et al., 2019).
FTIR spectra in triple bond spectral region (2000–2500 cm^{-1}) reveals characteristic C≡C stretching vibrations, indicative to unsaturated hydrocarbons and minor lipid components. These observations align with Durak and Durak (2021), who demonstrated that lipid unsaturation enhances membrane fluidity and supports adaptive physiological responses during insect development. Although these peak intensities remained relatively stable across instars, their persistent presence shows the functional role of a hydrocarbon backbone in maintaining both membrane and cuticular integrity. In double bond region (1500–2000 cm^{-1}), carbonyl stretching vibrations observed near 1749 cm^{-1} indicate the presence of lipid and phospholipid moieties. Notably, the increased intensity at later instars reflects to lipid accumulation to aid later developmental energy requirements. This pattern corroborates previous studies in aphid species, where lipid-specific absorption peaks around 1737 cm^{-1} correspond to wax ester and cuticular lipid variations (Durak et al., 2024). Furthermore, the amide I (1643 cm^{-1}) and amide II (1559 cm^{-1}) peaks exhibited increased protein concentration towards pupation, indicating structural and enzymatic protein remodeling and activity. Similar changes were noted in differentiating developmental stages of fly larvae (Pickering et al., 2015) and in mosquito populations analyzed by NIRS (Sikulu-Lord et al., 2016).
The fingerprint region (600–1500 cm^{-1}) provides critical insights into the structural and metabolic composition of larval hemolymph. Absorption bands at 1396 and 1367 cm^{-1} are assigned to –COO symmetric stretching and C–H bending vibrations, indicating the presence of fatty acid moieties and amide III contributions associated with protein secondary structures. Additionally, peaks at 1167–1172 cm^{-1} and 1088–1089 cm^{-1} correspond to C–O and PO_2 stretching vibrations, confirming the presence of phospholipids, carbohydrates (particularly trehalose) and nucleic acid components. These biochemical constituents play pivotal roles in energy metabolism and cellular regulation during insect development. The prominence of trehalose aligns with findings of Sinclair (2015) and Mwanga et al. (2019), who emphasized the metabolic significance of trehalose (blood sugar in insects) and associated phospholipids in insect developmental physiology.
The progressive enhancement of protein and lipid components from the third to fifth instar reflects a metabolic shift from carbohydrate-dominant to protein- and lipid-rich hemolymph, corresponding with the physiological preparation for pupation. This biochemical progression aligns with earlier spectroscopic analyses across insect taxa that demonstrated increasing protein and lipid accumulation during late larval instars (Dowell et al., 1999; Johnson, 2020; Fernandes et al., 2018). ATR-FTIR spectroscopy successfully detected biochemical markers to identify flunitrazepam residues in necrophagous flies across life stages (Oliveira et al., 2014; Baia et al., 2016) and differentiate species within orders Diptera and Lepidoptera (Jia et al., 2007; Siegwart et al., 2015). Similarly, spectroscopic method used to differentiate sex in fly pupae (Dowell et al., 2005), identify storage pests (Dowell et al., 1999), and discrimination of genetically or morphologically similar species (Fischaller et al., 2012; Barbosa et al., 2018). Beyond taxonomy, ATR-FTIR spectroscopy employed to investigate forensic entomology, disease vector identification, and pest management. Fernandes et al. (2018) spotted Zika virus in *Aedes aegypti*, while Khoshmanesh et al. (2017) identified Wolbachia endosymbionts in the mosquito species. Sikulu-Lord et al. (2016) demonstrated that NIRS can quickly anticipate the age of both wild-type and Wolbachia-infected *A. aegypti*, and Maia et al. (2019) applied to detect *Plasmodium falciparum* infections in *Anopheles gambiae*. Collectively, the distinct spectral markers identified for each instar highlight its versatile applications in age grading, species differentiation, and developmental staging (Ong et al., 2020; Mwanga et al., 2019).

4. CONCLUSION

In conclusion, ATR-FTIR spectroscopy emerged as a rapid, non-destructive, reliable technique for characterizing instar-specific biochemical changes in the hemolymph of *S. frugiperda*. The distinct spectral signatures observed in 3rd, 4th, and 5th larval instars correspond to key physiological and metabolic transitions associated with larval growth and development. These findings exhibit the prospects of ATR-FTIR spectroscopy as a valuable tool in entomological diagnostics and developmental biology, offering a robust platform for monitoring biochemical and metabolic changes during insect development.

Acknowledgement
Authors acknowledge the support of Director, ICAR-National Institute of Biotic Stress Management, Raipur, Chhattisgarh, for providing all the necessary facilities and support to carry out this study.

Conflict of Interest
The Author declares that they have no conflict of interest.

Author's Contribution Statements
S. Maheshwari conducted the research work, curated the data, and wrote the original draft. K. C. Sharma contributed to conceptualization, resources, supervision, writing the original draft, and manuscript review and editing. S. K. Jain contributed resources and supervision. P. Meena manuscript review and editing. P. Kekti and G. Songer contributed to writing the draft, manuscript review, and editing. T. Nayak contributed to analysis, writing the original draft, and manuscript review and editing. H. P. Verma contributed to writing the draft and manuscript review and editing. P. K. Rai provided overall supervision, visualization, resources, and project administration. All authors have read and agreed to the published version of the manuscript

REFERENCES

1. Akiki, P., Delamotte, P., & Montagne, J. (2024). Lipid metabolism in relation to carbohydrate metabolism. In: A. G. woods and C.C. Darie (Ed.) Advances in Experimental Medicine and Biology (pp. 239-259). Springer, Cham. https://doi.org/10.1007/5584_2024_821
2. Bagnères, A. G. and Wicker-Thomas, C. (2010). Chemical taxonomy with hydrocarbons (pp. 121-162). Cambridge University Press, Cambridge, Massachusetts. https://doi.org/10.1017/CBO9780511711909.008
3. Baia, F. A., Oliveira, J. A., dos Santos, A. L. and de Carvalho Queiroz, M. M. (2016). Spectroscopic detection of flunitrazepam in necrophagous fly species. Forensic Sci. Int., 266, 530–535. https://doi.org/10.1016/j.forsciint.2016.07.003
4. Barbosa, R. R., Rohwedder, A., Lima, S. M. and Antonialli-Junior, W. F. (2018). Infrared spectroscopic identification of Sarcophagidae species (Diptera). J Forensic Sci., 63(3), 821–827. https://doi.org/10.1111/1556-4029.13663
5. Boulet-Audet, M., Vollrath, F. and Holland, C. (2015). Identification and classification of silks using infrared spectroscopy. J. Exp. Biol., 218(19), 3138- 3149.
6. Browne, N., Heelan, M. and Kavanagh, K. (2013). An analysis of the structural and functional similarities of insect hemocytes and mammalian phagocytes. Virulence., 4(7), 597-603. https://doi.org/10.4161/viru.25906
7. Coates, J. (2000). Interpretation of Infrared Spectra—A Practical Approach. In R.A. Meyers (Ed.), Encyclopedia of Analytical Chemistry (pp. 10815–10837). Chichester: John Wiley & Sons Ltd. https://doi.org/10.1002/9780470027318.a5606
8. Cozzolino, D. (2014). An overview of the use of infrared spectroscopy and chemometrics in authenticity and traceability of cereals. Food Res. Int., 60, 262- 265. https://doi.org/10.1016/j.foodres.2013.08.034
9. Dowell, F. E., Nansen, C. and Perez-Mendoza, J. (2005). Gender determination of fly pupae using near-infrared spectroscopy. J. Stored Prod. Res., 41(2), 197–204. https://doi.org/10.1016/j.jspr.2004.03.004
10. Dowell, F. E., Throne, J. E., Wang, D. and Baker, J. E. (1999). Identifying stored- grain insects using near-infrared spectroscopy. J. Econ. Entomol., 92(1), 165–169. https://doi.org/10.1093/jee/92.1.165
11. Durak, R., and Durak, T. (2021). The significance of cuticular lipids in the survival of insects. Insect Biochem. Mol. Biol., 127, 103512. https://doi.org/10.1016/j.ibmb.2020.103512
12. Durak, R., Durak, T. and Kot, I. (2024). Lipid metabolism during diapause in aphids: A spectroscopic approach. Comp. Biochem. Physiol. B., 280, 110995. https://doi.org/10.1016/j.cbpb.2024.110995
13. Wronska, A. K., Kaczmarek, A., Boguś, M. I. and Kuna, A. (2023). Lipids as a key element of insect defense systems. Front. Genet., 14, 1183659. 10.3389/fgene.2023.1183659
14. Charles, J. P. (2010). The regulation of expression of insect cuticle protein genes. Insect biochem. Mol. Biol., 40(3), 205-213. https://doi.org/10.1016/j.ibmb.2009.12.005
15. Lehmann, M. (2021). Diverse roles of phosphatidate phosphatases in insect development and metabolism. Insect Biochem. Mol. Biol., 133, 103469. https://doi.org/10.1016/j.ibmb.2020.103469
16. Eleftherianos, I., Heryanto, C., Bassal, T., Zhang, W., Tettamanti, G. and Mohamed, A. (2021). Hemocyte-mediated immunity in insects: Cells, processes and associated components in the fight against pathogens and parasites. Immunology., 164(3), 401–432. https://doi.org/10.1111/imm.13404
17. Ellis, D. I., Harrigan, G. G. and Goodacre, R. (2003). Metabolic fingerprinting with Fourier transform infrared spectroscopy. In Metabolic Profiling: Its Role in Biomarker Discovery and Gene Function Analysis (pp. 111–124). Springer US. https://doi.org/10.1007/978-1-4419-8983-7_7
18. Fernandes, J., Maia, M. F., Sikulu-Lord, M. T. and Hugo, L. E. (2018). Infrared spectroscopic detection of Zika virus in Aedes aegypti. Anal. Chem., 90(12), 7220–7226. https://doi.org/10.1021/acs.analchem.8b00923
19. Fischaller, M., Ritz, C. and Kostal, V. (2012). Species discrimination in Drosophila obscura group using infrared spectroscopy. Anal. Bioanal. Chem., 403(1), 45–52. https://doi.org/10.1007/s00216-012-5788-1
20. Gibbs, A. and Crowe, J. H. (1991). Intra-individual variation in cuticular lipids studied using Fourier transform infrared spectroscopy. J. Insect Physiol., 37(10), 743-748. https://doi.org/10.1016/0022-1910(91)90108-C
21. Gonzalez-Jimenez, M., Babayan, S. A., Khazaeli, P., Doyle, M. Walton, F., ……Wynne, K. (2019). Prediction of mosquito age, species, and population age structure using mid-infrared spectroscopy and supervised machine learning. Wellcome Open Res., 4, 76.
22. Gupta, A. P. (2019). Insect immunocytes and other hemocytes: Roles in cellular and humoral immunity. In Immunology of insects and other arthropods (pp. 19– 118). CRC Press.
23. Horvatinec, J. and Svečnjak, L. (2020). Infrared (FTIR) spectral features of honey bee (Apis mellifera L.) hemolymph. J. Cent. Eur. Agric., 21(1), 37–41. https://doi.org/10.5513/JCEA01/21.1.2569
24. Jia, F., Zhang, H. and Liu, W. (2007). Identification of Lepidoptera species using spectrophotometric techniques. Appl. Entomol. Zool., 42(4), 573–579. https://doi.org/10.1303/aez.2007.573
25. Johnson, J. B. and Naiker, M. (2020a). Mid-infrared spectroscopy for entomological purposes: A review. J. Asia-Pac. Entomol., 23(3), 613–621. https://doi.org/10.1016/j.aspen.2020.03.015
26. Johnson, J. B. and Naiker, M. (2020b). Seeing red: A review of the use of near- infrared spectroscopy (NIRS) in entomology. Appl. Spectrosc. Rev., 55(9-10), 810-839. https://doi.org/10.1080/05704928.2019.1685532
27. Johnson, J., Collins, T., Skylas, D. and Naiker, M. (2019). ATR-MIR: A valuable tool for the rapid assessment of biochemically active compounds in grains. In 69th Australasian Grain Science Conference, Carlton, Melbourne, Australia (pp. 27- 29).

28. Johnson, S. D. (2020). Use of infrared spectroscopy to identify leafhopper species within Hemiptera. Entomol. Res., 50(1), 1–9. https://doi.org/10.1111/1748- 5967.12418
29. Khoshmanesh, A., Christensen, D., Perez-Guaita, D., Iturbe-Ormaetxe, I., O'Neill, S. L., McNaughton, D. and Wood, B. R. (2017). Screening of Wolbachia endosymbiont infection in Aedes aegypti mosquitoes using attenuated total reflection mid-infrared spectroscopy. Anal. Chem., 89(10), 5285-5293. https://doi.org/10.1021/acs.analchem.6b04827
30. Kuroiwa, D. R., Max, J. J. and Chapados, C. (2015). Vibrational spectroscopy of aqueous carbohydrate solutions. J. Phys. Chem. B., 119(31), 9923–9932. https://doi.org/10.1021/acs.jpcb.5b05828
31. Lavine, M. D. and Strand, M. R. (2002). Insect hemocytes and their role in immunity. Insect Biochem. Mol. Biol., 32(10), 1295–1309. https://doi.org/10.1016/S0965-1748(02)00092-9
32. Maia, M. F., Fernandes, J., Sikulu-Lord, M. T. and Hugo, L. E. (2019). Detection of Plasmodium falciparum-infected Anopheles gambiae using near-infrared spectroscopy. Anal. Chemistry., 91(15), 9632–9639. https://doi.org/10.1021/acs.analchem.9b01075
33. Maranabasari, S., Deshmukh, S. S., Kalleshwaraswamy, C. M., Veeranna, H. K., and Thippeshappa, G. (2024). Efficacy of seed treatment with diamides against fall armyworm, Spodoptera frugiperda (JE Smith) in early stage of the maize crop. J. Entomol. Res., 48(4), 443-448.
34. Mullins, D. E. (2013). Chemistry and physiology of the hemolymph. In: Comprehensive Insect Physiology, Biochemistry and Pharmacology (Vol. 3, pp.355–400). Elsevier. https://doi.org/10.1016/B978-0-08-092323-1.65152-9
35. Mwanga, E. P., Kaindoa, E. W., Ngowo, H. S., Mapua, S. A., Matowo, N. S. and Koekemoer, L. L. (2019). Mid-infrared spectroscopy accurately identifies vertebrate blood meals in malaria vectors. Scientific Reports., 9(1), 1538. https://doi.org/10.1038/s41598-018-38251-2
36. Nandiyanto, A. B. D., Oktiani, R. and Ragadhita, R. (2019). How to read and interpret FTIR spectroscope of organic material. Indones. J. Sci. Technol., 4(1), 97-118. https://doi.org/10.17509/ijost.v4i1.15806
37. Oliveira, J. A., Baia, F. A. and de Carvalho Queiroz, M. M. (2014). Detection of chemical compounds in fly larvae using spectroscopic methods. Forensic Sci. Int., 238, 45–51. https://doi.org/10.1016/j.forsciint.2014.02.013
38. Ong, P. L., Sikulu-Lord, M. T., Hugo, L. E. and Wood, O. (2020). Near-infrared spectroscopy predicts mosquito age and infection status. J. Vector Ecol., 45(1), 34–42. https://doi.org/10.1111/jvec.12369
39. Paikra, S. and Mishra, M. (2019). Fourier Transform Infrared Spectroscopy: A novel approach for biomolecular characterization of Drosophila hemolymph. In Fundamental Approaches to Screen Abnormalities in Drosophila (pp. 209–222). Springer US. https://doi.org/10.1007/978-1-4939-9107-2_12
40. Pickering, J., Mabhula, A. and van der Lingen, C. D. (2015). The use of FTIR spectroscopy for species and life stage identification in Diptera. Forensic Sci. Int., 249, 311–320. https://doi.org/10.1016/j.forsciint.2015.02.016
41. Rodriguez-Saona, L. E. and Allendorf, M. E. (2011). Use of FTIR for rapid authentication and detection of adulteration of food. Annu. Rev. Food Sci. Technol., 2(1), 467-483.
42. Siegwart, M., Bouvier, F., Maugin, S., Lecomte, A. and Lavigne, C. (2015). Differentiating oriental fruit moth and codling moth (Lepidoptera: Tortricidae) larvae using near-infrared spectroscopy. J. Econ. Entomol., 108(1), 219-227. https://doi.org/10.1093/jee/tou020
43. Sikulu-Lord, M. T., Henry, M., Mayagaya, V. S. and Hugo, L. E. (2016). Rapid age grading of Aedes aegypti using near-infrared spectroscopy. PLOS Negl. Trop. Dis., 10(10), e0005121, https://doi.org/10.1371/journal.pntd.0005121
44. Sinclair, B. J. (2015). Linking energetics and overwintering in insects: Cuticular lipids and diapause. J. Insect Physiol., 81, 84–92. https://doi.org/10.1016/j.jinsphys.2015.06.001
45. Kalleshwaraswamy, C. M., Maruthi, M. S., and Pavithra, H. B. (2018). Biology of invasive fall army worm Spodoptera frugiperda (JE Smith) (Lepidoptera: Noctuidae) on maize. Indian J. Entomol., 80(3), 540-543. https://doi.org/10.5958/0974-8172.2018.00238.9
46. Tay, W. T., Meagher Jr, R. L., Czepak, C. and Groot, A. T. (2023). Spodoptera frugiperda: Ecology, evolution, and management options of an invasive species. Annu. Rev. Entomol., 68(1), 299–317.
47. Teixeira, R., Fernández, J. I. R., Pereira, J. and Monteiro, L. B. (2015). Identification of Grapholita molesta (Busk)(Lepidoptera: Tortricidae) biotypes using infrared spectroscopy. Neotrop. Entomol., 44(2), 129-133.
48. Wang, X., Kang, T. and Liu, H. (2017). Hemolymph in insect immunity. Dev. Comp. Immunol., 73, 81–89. https://doi.org/10.1016/j.dci.2017.01.021
49. Wang, Y., Nansen, C. and Zhang, Y. (2016). Integrative insect taxonomy based on morphology, mitochondrial DNA, and hyperspectral reflectance profiling. Zool. J. Linn. Soc., 177(2), 378-394. https://doi.org/10.1111/zoj.12367

Table 1. Characteristics of the ATR-FTIR spectrum of the fall armyworm hemolymph (spectral range: 4000-400 cm-1) with assignment of spectrum region, peaks observed at corresponding wavenumber, vibrational mode, functional group/assignment, and aetiological compound

Sl. No.	Mid-IR Spectrum region	Range (cm-1)	Peak observed at corresponding Wavenumber (cm-1) for larval hemolymph			Functional group /Assignment	Vibration mode	Aetiological Compound (s)
			3rd instar	4th instar	5th instar			
1.	Single bond region (2500-4000 cm-1)	3700-3800	3836.67	3836.67	3924.26	-OH (free hydroxyl, water, carbohydrates, protein)	Stretching	Hydrocarbon
2.		3600-3800	3801.08	3800.92	3899.43	-NH (Amide A), -OH overlapping	Stretching	Amide, Hydroxyl compound
3.		3500-3700	3742.40	3742.45	3836.76	Free -OH/moisture	Stretching	Hydroxyl compound
4.		3300-3700	3671.26	3671.10	3801.00	H-bonded OH/NH		Amide, Hydroxyl compound
5.		3400-3500	-	-	3742.32	-NH (proteins, Amides)	Stretching	Amides
6.		3200-3400	-	-	3671.37	Amide /water-bound -OH		Amides
7.		3200-3300	3284.47	3309.54	3312.99	-NH (protein), -OH of water and sugars	Bending	Carbohydrate, Amide & Hydroxyl group
8.	Triple Bond region (2000-2500 cm-1)	2000-2500	2119.36	2109.73	2120.00	-C≡C- (weak, possibly CO2)	-	-
9.	Double bond region (1500-2000 cm-1)	1500-2000	1867.06	1867.09	1867.21	Combination region	-	-
10.		1700-1750	1749.34	1749.51	1749.39	-C≡O- stretching of esters (Lipids, phospholipids)	Stretching	Esters, lipids, phospholipids, fatty acid
11.		1600-1700	1643.56	1643.09	1643.62	Amide I (-C≡O- stretch in proteins) bound water	Stretching	Primary Amides
12.		1500-1600	1559.91	1559.87	1559.85	Amide II (N-H bend along with - C-N- stretch)	Stretching	Secondary Amides
13.	Fingerprint region (600-1500 cm-1)	1500-1550	1523.40	1523.41	1523.36	-C-C- stretch (aromatic), CH2 bending	Stretching, bending	Aliphatic hydrocarbons
14.		1400-1450	1396.72	1396.83	1396.62	-COO- symmetric (amino acids, fatty acids)	Stretching	Amides
15.		1300-1400	1367.72	1367.49	1367.62	-C-H bending, Amide III	Bending	Tertiary Amides
16.		1150-1250	1167.47	1171.69	1172.06	-C-O- stretching, -PO-2 (Phospholipids, sugar)	Stretching	Phospholipids, carbohydrates

17.		1000-1100	1089.20	1089.36	1088.96	-C-O stretch of carbohydrates (trehalose), - PO - symmetric stretch 2 (Nucleic acids, Phospholipids)		Phospholipids, carbohydrates

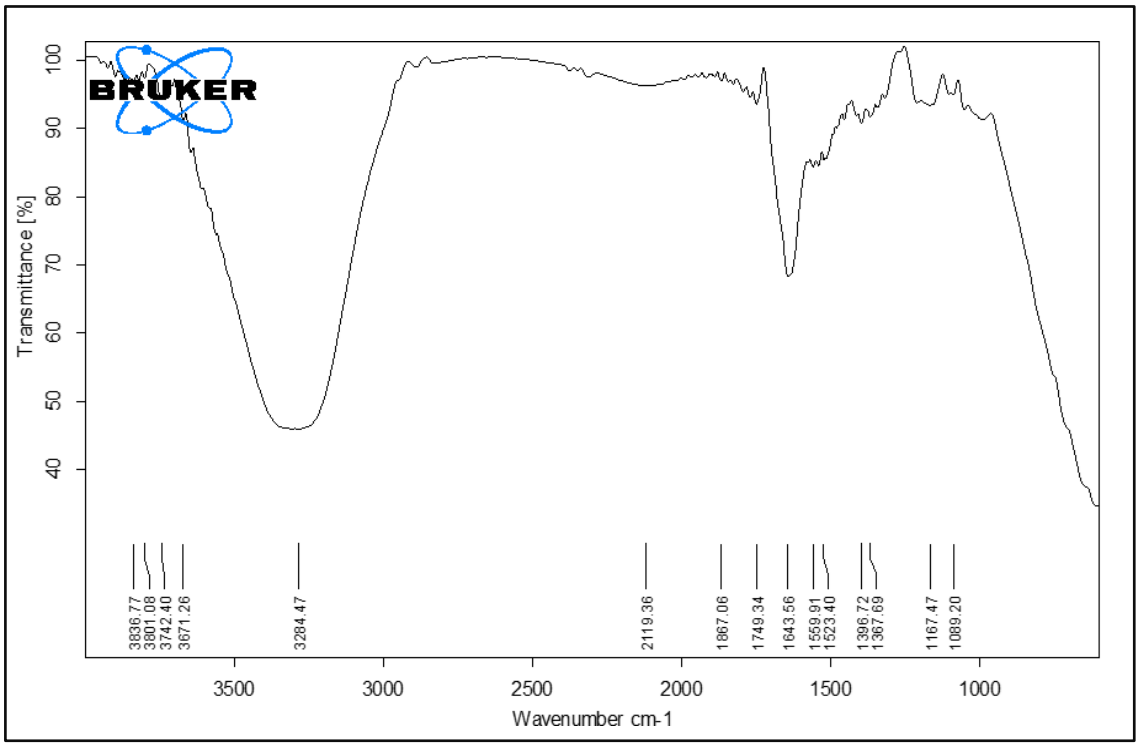

Fig. 1(a) 3rd instar larva

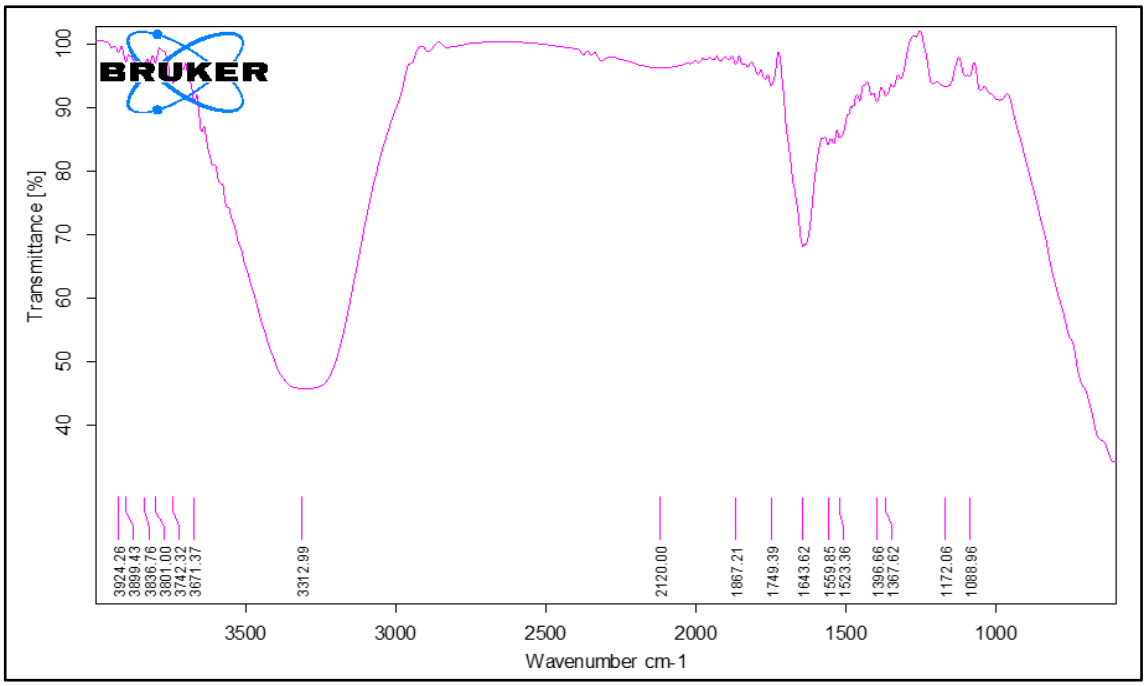

Fig. 1(b) 4th instar larva

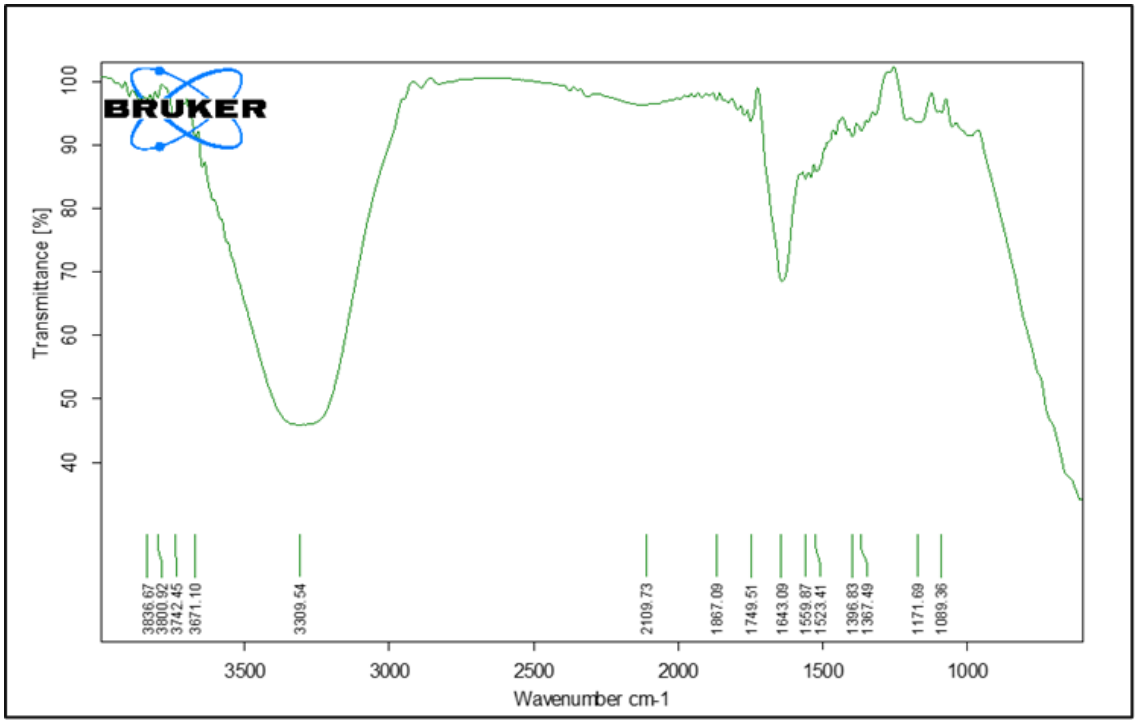

Fig. 1(c) 5th instar larva

Figure 1: ATR-FTIR spectrum of fall armyworm hemolymph (Spectral range: 4000-400 cm-1)